# Unimolecular Reactions of Proton-Bound Cluster Ions: Competition between Dissociation and Isomerization in the Ethanol−Acetonitrile Dimer

**Richard A. Ochran, Alagappan Annamalai,† and Paul M. Mayer***

*Chemistry Department, University of Ottawa, Ottawa, Canada K1N 6N5*

*Received: March 21, 2000; In Final Form: June 15, 2000*

The proton-bound dimer of acetonitrile and ethanol, $(CH_3CN)(CH_3CH_2OH)H^+$, exhibits three unimolecular reactions on the microsecond time scale: two simple bond cleavage reactions to form $CH_3CNH^+ + CH_3CH_2OH$ and $CH_3CH_2OH_2^+ + CH_3CN$, and the loss of water to form $CH_3CNCH_2CH_3^+$. The latter process is preceded by the isomerization of the proton-bound dimer to a second isomer, $(CH_3CNCH_2CH_3)(H_2O)^+$. The competition between the simple dissociation reactions and the isomerization reaction was modeled with ab initio calculations and RRKM theory to obtain relative energies for the reaction surface. The 0 K binding energy of the $(CH_3CN)(CH_3CH_2OH)H^+$ complex was calculated to be 152 kJ mol$^{-1}$ at the G2(MP2,SVP) level of theory (relative to the dissociation products $CH_3CNH^+$ and $CH_3CH_2OH$). The isomerization barrier for the proton-bound dimer was estimated to be 22 kJ mol$^{-1}$ lower than $CH_3CNH^+ + CH_3CH_2OH$. The greater polarizability of the ethyl group is believed to stabilize this transition structure over that found for the $(CH_3CN)(CH_3OH)H^+$ ion (which was previously estimated to lie 6 kJ mol$^{-1}$ below $CH_3CNH^+$ and $CH_3OH$).

## 1. Introduction

Cluster ions can range in size from simple dimers such as $(He)_2^+$ to large polymolecular species such as water hydrates, $H_3O^+(H_2O)_n$. Interest in their chemistry stems from their occurrence in the earth's atmosphere and in the study of the early stages of the effects of solvation. A central issue when studying the chemistry of gaseous ions is their propensity for rearrangement prior to reaction. Over the years, a variety of thermodynamically stable structures have been discovered including distonic ions,[1] ion/neutral complexes,[2,3] and bridged ions.[4] These ion structures are ubiquitous to ion dissociation mechanisms, and indeed, the isomerization of gas-phase organic ions appears to be a common occurrence.[5−9] However, the isomerization reactions of cluster ions have not been extensively studied.[10−12]

We began studying proton-bound dimers in order to identify possible rearrangements that occur in the course of their unimolecular reactions. The family of proton-bound mixed dimers consisting of nitriles and alcohols all have at least one common feature: they exhibit in their unimolecular chemistry the competition between simple bond dissociations and dehydration reactions. In this respect, they are similar to many proton-bound alcohol dimers.[13−18] Recent work in our laboratory[19] showed that the metastable proton-bound dimer of acetonitrile and methanol, $(CH_3CN)(CH_3OH)H^+$, undergoes two unimolecular reactions on the microsecond time scale, a simple bond cleavage reaction to form $CH_3CNH^+$ and $CH_3OH$, and the loss of water to form $CH_3CNCH_3^+$. The water loss channel is preceded by rearrangement of the proton-bound dimer to a second isomer, $(CH_3CNCH_3)(H_2O)^+$. The reaction surface derived for this system is reproduced in Figure 1. The other alcohol−acetonitrile clusters also exhibit this competition of simple bond cleavage reactions and dehydration reactions, but to varying extents. The competition between the two channels means that there is a fine balancing of the thresholds for dissociation with the barriers to isomerization.

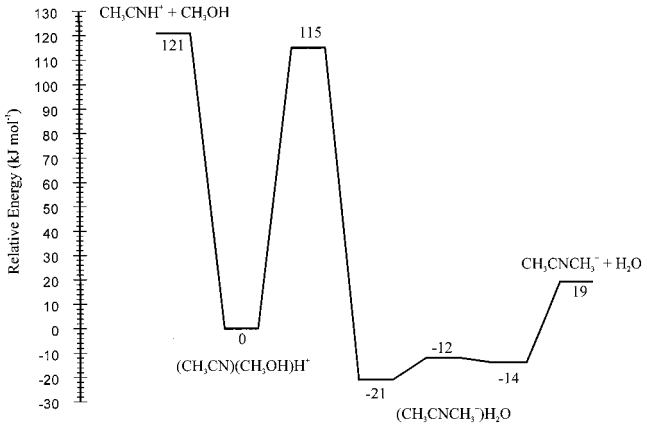


**Figure 1.** Potential energy surface for the unimolecular dissociations of the proton-bound dimer $(CH_3CN)(CH_3OH)H^+$.[19] All values in kJ mol$^{-1}$.

The present study concerns itself with the next member of this family of proton-bound dimers, that between acetonitrile and ethanol, $(CH_3CN)(CH_3CH_2OH)H^+$. In it, we identify the key features of the potential energy surface using mass spectrometry and ab initio theory and compare the surface to its methanol homologue.

## 2. Experimental Procedures

The experiments were performed on a modified triple sector VG ZAB-2HF mass spectrometer[20] incorporating a magnetic sector followed by two electrostatic sectors (BEE geometry). Protonated cluster ions were generated in the chemical ionization ion source of the instrument. The pressures in the ion source chamber, read with an ionization gauge located above the ion source diffusion pump, were typically between $10^{-5}$ and $10^{-4}$ Torr (the pressure in the ion source itself being approximately

* Corresponding author. E-mail: pmayer@science.uottawa.ca.
† Undergraduate researcher.

10.1021/jp001051l CCC: $19.00 
Published on Web 08/24/2000

2 orders of magnitude higher). Cluster ions were not observed when the pressure was below $10^{-5}$ Torr, and there was no evidence of higher order clusters at any of the pressures used in these experiments. Metastable ion (MI) and collision-induced dissociation (CID) mass spectra were recorded in the usual manner in both the second and third field-free regions (2FFR and 3FFR, respectively) of the instrument.[21] Helium collision gas was used in all CID experiments and was introduced into the collision cells to achieve 10% reduction in the ion flux (i.e., single collision conditions). All chemicals were commercially obtained and used without further purification. Isotopically labeled compounds (MSD Isotope Ltd.) were of 99% purity.

### 3. Computational Procedures

Standard ab initio molecular orbital calculations[22] were performed using the Gaussian 94[23] and 98[24] suites of programs. Geometries were optimized, and harmonic vibrational frequencies were calculated, at both the HF/6-31G(d) and MP2/6-31+G(d) levels of theory. Two recent assessments of theoretical procedures for calculating the properties of proton-bound dimers involving HCN and $CH_3CN$ with a variety of first-row hydrides have shown that geometries optimized at the MP2/6-31+G(d) level of theory provide an adequate foundation for high level single-point energy calculations.[25,26] Relative energies have also been found to be reasonably estimated at this level.[27]

Single-point energies on the MP2/6-31+G(d) geometries were obtained at the G2(MP2,SVP)[28] level of theory. Our previous assessments[25,26] showed that reasonable cluster binding energies and heats of formation can be calculated at this level of theory. G2(MP2,SVP) approximates the QCISD(T)/6-311+G(3df,2p) single-point energy by two additive corrections to a base MP2/6-31G(d) energy. The first is a basis set correction relative to the MP2/6-311+G(3df,2p) energy, and the second is an electron-correlation correction relative to QCISD(T)/6-31G(d). This final total energy is then corrected further with an empirical higher-level correction which attempts to account for residual basis set deficiencies in the above total energy, and also with the zero-point vibrational energy (ZPE). The ZPE used in G2(MP2,-SVP) is the HF/6-31G(d) value scaled by 0.8929.

Thermal corrections to the data were carried out using MP2/6-31+G(d) vibrational frequencies (scaled by 0.9434).[29] Theoretical heats of formation ($\Delta_f H°$) were derived by the atomization method employing experimental heats of formation of the constituent atoms.[30]

### 4. Results and Discussion

**Mass Spectrometry.** *Metastable $(CH_3CN)(CH_3CH_2OH)H^+$ Ions*. The 2FFR MI mass spectrum (Figure 2a) of the proton-bound dimer $(CH_3CN)(CH_3CH_2OH)H^+$ (**I**) *m/z* 88, exhibits three peaks, *m/z* 70 (−18 amu), *m/z* 47 (−41 amu), and *m/z* 42 (−46 amu) having relative intensities of 1:0.21:0.27. The loss of 18 amu to form *m/z* 70 can only be attributed to water loss, while the other two reactions can be attributed to the loss of acetonitrile (to form protonated ethanol) and ethanol (to form protonated acetonitrile), respectively. The identities of the metastably generated *m/z* 42 and *m/z* 47 ions were confirmed by transmitting them into the 3FFR and obtaining their CID mass spectra. These spectra were found to be identical to those of $CH_3CNH^+$ and $CH_3CH_2OH_2^+$ generated in the ion source by self-protonation. These two ions are likely generated from the proton-bound dimer by simple-bond cleavage reactions.

In the MI mass spectrum, the *m/z* 42 peak is only slightly more intense than the *m/z* 47 peak (1.3:1), which is consistent with the relative proton affinities (PA) of acetonitrile and ethanol. The most recent critically evaluated compendium lists the PA of $CH_3CN$ to be 779.2 kJ $mol^{-1}$ and that of $CH_3CH_2OH$ to be 776.4 kJ $mol^{-1}$.[31] The difference in intensities is more pronounced in the MI mass spectrum of the dimer obtained in the 3FFR (and hence at a longer time scale) where the relative intensities of *m/z* 70, 47, and 42 are 1:0.11:0.24. Introduction of a trace amount of collision gas into a collision cell results in a dramatic increase in the intensities of *m/z* 42 and *m/z* 47 relative to *m/z* 70, the latter being largely unaffected. This suggests that the dissociation channel leading to *m/z* 70 involves a rearrangement of the initially generated proton-bound dimer. In this respect, the results are analogous to those of the methanol−acetonitrile proton-bound dimer ion.[19] The kinetic energy release (KER) values for the competing processes (dissociation and rearrangement, reported from the full width at half-height of the three peaks, $T_{0.5}$) are 18 meV (*m/z* 42), 11 meV (*m/z* 47), and 26 meV (*m/z* 70). The first two values are typical values for simple bond dissociation reactions, while the latter is consistent with the dissociation of a weakly bound species (and is similar to that observed for the methanol-acetonitrile dimer).[19]

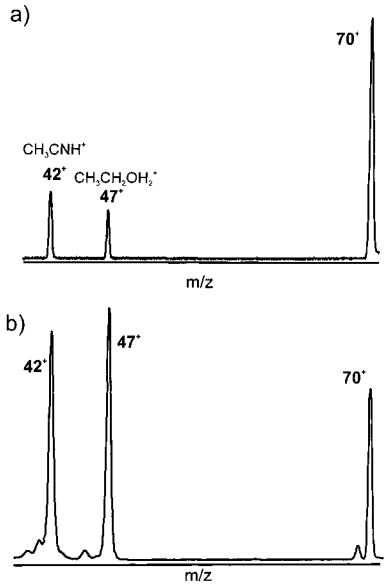


**Figure 2.** (a) MI mass spectrum of $(CH_3CN)(CH_3CH_2OH)H^+$ obtained in the second field-free region of the VG ZAB-2HF, (b) CID mass spectrum of $(CH_3CN)(CH_3CH_2OH)H^+$ obtained in the second field-free region of the VG ZAB-2HF.

*Collisionally Excited $(CH_3CN)(CH_3CH_2OH)H^+$ Ions*. The CID mass spectrum of the *m/z* 88 ions (Figure 2b) shows a substantial increase in the intensities of $CH_3CNH^+$ and $CH_3CH_2OH_2^+$ (*m/z* 42 and 47, respectively) relative to *m/z* 70 (water loss). This is again consistent with the latter channel involving a rearrangement of the initially formed proton-bound dimer. The relative intensities of the two simple bond cleavage reaction products, however, are inverted in the CID mass spectrum, with *m/z* 47 being more intense than *m/z* 42. Typically, when a proton-bound dimer dissociates by two competing simple bond cleavage reactions, it is assumed that the two channels are characterized by similar entropies of activation, $\Delta S^{\ddagger}$. The result is that upon collisional activation, the relative intensities of the peaks in the mass spectrum corresponding to the two cleavage reactions become more similar, but do not invert.[32] The present result indicates that these two dissociation channels may be characterized by different entropies of activation (see discussion of RRKM modeling).

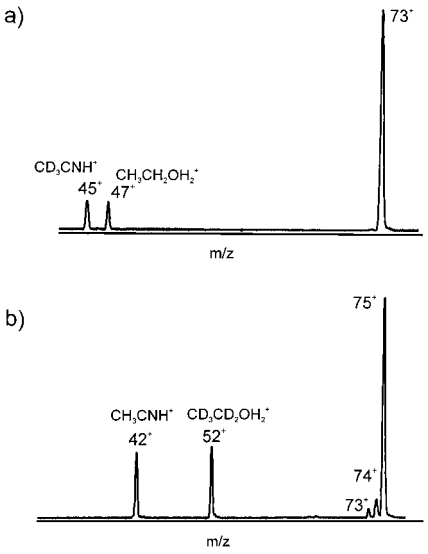


**Figure 3.** (a) MI mass spectrum of the isotopically labeled ion $(CD_3CN)(CH_3CH_2OH)H^+$ and (b) MI mass spectrum of the isotopically labeled ion $(CH_3CN)(CD_3CD_2OH)H^+$, obtained in the 2FFR of the instrument.

*Identity of m/z 70*. The CID mass spectra of source generated *m*/*z* 70 and metastably generated *m*/*z* 70 were found to be identical. The MI mass spectrum of source generated *m*/*z* 70 ions exhibits one peak at *m*/*z* 42 which was confirmed to be protonated acetonitrile. A collision-induced dissociation ionization (CIDI)[33] experiment was performed in order to identify the neutral species accompanying this dissociation. The mass spectrum exhibits four consecutive peaks from *m*/*z* 25 through *m*/*z* 28, indicating that the neutral lost is $C_2H_4$ and not CO or HCNH. Based on these data, and from analogy to the methanol-acetonitrile dimer ion reaction surface, we propose two possible isomers for *m*/*z* 70: $CH_3CNCH_2CH_3^+$ (**II**) and $(CH_3CN)(C_2H_4)H^+$ (**III**).

*Isotopic Labeling Studies.* Isotopically labeled cluster ions were studied to determine the extent of interchange of the hydrogen atoms in the proton-bound dimer. The cluster ions $(CD_3CN)(CH_3CH_2OH)H^+$ (*m*/*z* 91, formed by the reaction of $CD_3CN$ with $CH_3CH_2OH$ in the ion source) exhibit three fragment ion peaks in their MI mass spectrum, *m*/*z* 73 (−18 amu), *m*/*z* 47 ($CH_3CH_2OH_2^+$), and *m*/*z* 45 ($CD_3CNH^+$), Figure 3a. The identities of these ions were confirmed by their CID mass spectra. These observations indicate that there is no mixing of the methyl hydrogens on acetonitrile with those of the bridging hydrogens (the $H^+$ bridge and hydroxy hydrogen) or those on the ethyl group.

Ethanol-$d_5$ was introduced into the ion source and reacted with $CH_3CN$ to form *m*/*z* 93 $(CH_3CN)(CD_3CD_2OH)H^+$. The MI mass spectrum contained five peaks, *m*/*z* 42 ($CH_3CNH^+$), *m*/*z* 52, ($CD_3CD_2OH_2^+$), and a set of peaks with *m*/*z* 73, 74, and 75 (Figure 3b). The latter three peaks represent the loss of $D_2O$, HOD, and $H_2O$, respectively, in the ratio 0.04:0.09:1.0. These results, coupled with those discussed above, show that a small amount of interchange occurs between the ethyl hydrogens and the bridge hydrogens, but that this mixing occurs only after isomerization of the originally formed proton-bound dimer. The results also show that this mixing is a minor process, with the initially formed isomer ion preferentially dissociating to lose $H_2O$.

*Summary of Experimental Results.* The experimental results are consistent with a two-well reaction surface similar to that proposed for the methanol−acetonitrile proton-bound dimer ion. It is clear from the isotopic labeling experiments that, while there appears to be secondary reactions after isomerization of the proton-bound dimer that result in some hydrogen exchange, these reactions do not compete favorably with dissociation to *m*/*z* 70 + $H_2O$.

**Ab Initio Calculations**. The mass spectrometric results indicate that there is likely to be a thermodynamically stable isomer or limited number of isomers in the reaction that are responsible for water loss. Ab initio calculations have been used to identify possible structures and model the reaction surface. Structures optimized at the MP2/6-31+G(d) level of theory can be found in Figure 4, and relative energies at this and the G2-(MP2,SVP) level of theory are listed in Table 1. Calculated heats of formation for all equilibrium species are compared to available experimental values in Table 2.

*Isomeric Forms of m/z 70*. Two stable isomers of *m*/*z* 70 were located: a covalently bonded structure, **II**, analogous with that found in the previous methanol−acetonitrile study,[19] and a proton-bound acetonitrile−ethene dimer, **III**. Ion **II** is calculated to be 99 kJ $mol^{-1}$ lower in energy than ion **III** at the G2(MP2,SVP) level of theory (Table 1). The transition structure for the interconversion of the two isomeric *m*/*z* 70 ions lies 58 kJ $mol^{-1}$ above ion **III**, and 8 kJ $mol^{-1}$ above the fragmentation products $CH_3CNH^+ + C_2H_4 + H_2O$. The height of this barrier suggests that while **II** may isomerize to **III** prior to metastable dissociation to $CH_3CNH^+$, the reverse isomerization is unlikely.

*Isomeric Forms of m/z 88.* A limited number of isomeric forms of the proton-bound dimer (**I**) were investigated in an attempt to model the reaction surface. Since *m*/*z* 70 is formed by the loss of water, probable candidates consisted of the above-mentioned *m*/*z* 70 isomer **II** with an electrostatically bound water molecule (Figure 4). Structures **IV** and **V** are ion−molecule complexes between $CH_3CNCH_2CH_3^+$ and $H_2O$. Other attempts involving moving the water to other locations all optimized to **IV**. The relative energies of these two isomers at the MP2 level of theory showed that **IV** and **V** were thermodynamically more stable than the proton-bound dimer, with **IV** being slightly lower in energy than **V** (Table 1). G2(MP2,SVP) level calculations put these two isomers slightly higher in energy than **I** (2 and 11 kJ $mol^{-1}$, respectively). As with the methanol−acetonitrile surface, it is expected that the barrier to interconversion of these two isomers is small.

Another possible series of isomers would consist of ion **III** with an electrostatically bound water, $(CH_3CN)(C_2H_4)(H_2O)H^+$. The energy relative to the proton-bound dimer of $(CH_3CN)(H_2O)H^+ + C_2H_4$ is calculated to be 90 kJ $mol^{-1}$ at the G2(MP2,SVP) level of theory. Since the binding energy of a molecule of ethene to $(CH_3CN)(H_2O)H^+$ is expected to be small, the formation of the $(CH_3CN)(C_2H_4)(H_2O)H^+$ isomer should be accompanied by the appearance of *m*/*z* 60, $(CH_3CN)(H_2O)H^+$, in the MI mass spectrum. The absence of *m*/*z* 60 in Figure 2 indicates that this isomerization channel is not a significant process.

*Isomerization Mechanism*. The isomerization from the proton-bound dimer to isomer **IV** likely involves the interconversion of a series of ion−dipole complexes in a mechanism that is similar to the $S_N2$-type mechanism that has been demonstrated for the proton-bound alcohol dimer ions.[34−36] The alcohol dimer mechanism consists of the backside attack of the neutral alcohol on the carbon adjacent to the $OH_2$ moeity in the protonated alcohol. Two stable intermediate complexes have been calculated in the case of the methanol dimer, $[CH_3O(H)\cdots CH_3OH_2]^+$

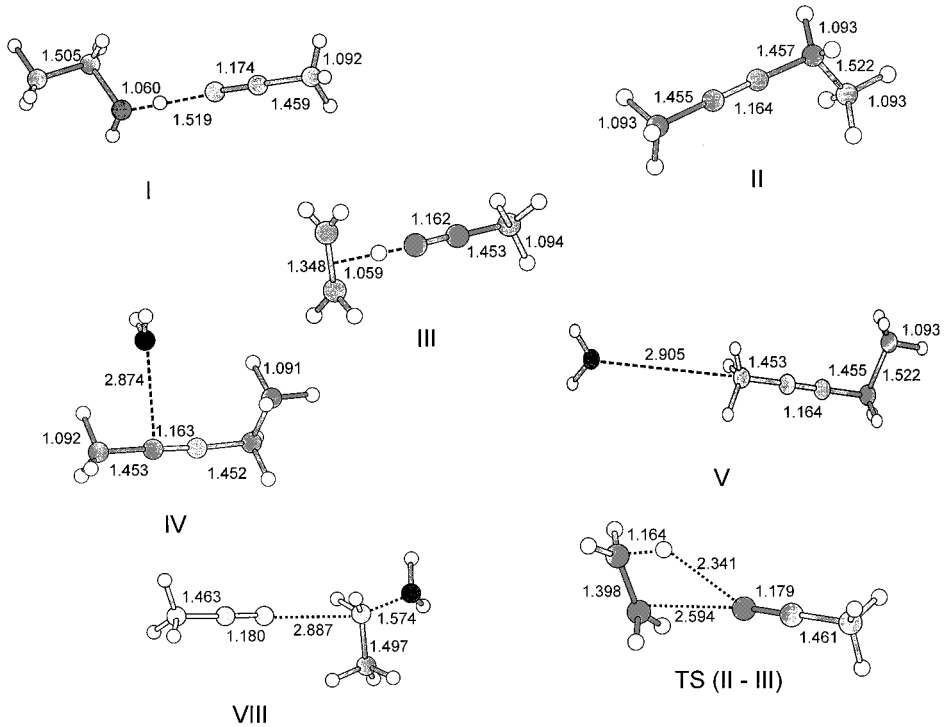


**Figure 4.** Selected geometric parameters for the proton-bound dimer $(CH_3CN)(CH_3CH_2OH)H^+$ (**I**) and isomers **IV**, **V**, and **VIII**, isomers of *m*/*z* 70, **II** and **III**, and the transition structure for their interconversion **TS(II → III)**. All geometries were fully optimized at the MP2/6-31+G(d) level of theory. Bond lengths are in angstroms, bond angles in degrees.

**TABLE 1: Calculated Relative Energies**

| ion | relative energy[a] | |
|---|---|---|
| | MP2/6-31+G(d) | G2(MP2,SVP) |
| I | 0 | 0 |
| IV | −8 | 2 |
| V | −7 | 11 |
| VIII | 75 | 96 |
| **II** + $H_2O$ | 31 | 42 |
| **III** + $H_2O$ | 142 | 141 |
| **TS(I → IV)** | 130[b] | 130[b] |
| **TS(II → III)** + $H_2O$ | 204 | 199 |
| $CH_3CNH^+ + CH_3CH_2OH$ | 139 | 152 |
| $CH_3CH_2OH_2+ + CH_3CN$ | 134 | 156 |
| $CH_3CNH^+ + C_2H_4 + H_2O$ | 194 | 191 |

[a] Values are in kJ mol$^{-1}$ at 0 K. [b] From RRKM modeling (see text).

**TABLE 2: Comparison of Calculated G2(MP2,SVP) and Experimental Heats of Formation[a]**

| species | $\Delta_f H°_0$ | $\Delta_f H°_{298}$ | LBLHLM[b] | NIST[c] |
|---|---|---|---|---|
| I | 460 | 433 | | |
| II | 741 | 720 | | |
| III | 841 | 823 | | |
| IV | 462 | 438 | | |
| V | 472 | 449 | | |
| VIII | 556 | 529 | | |
| $CH_3CN$ | 79 | 71 | 74 ± 1 | 74.04 ± 0.37 |
| $CH_3CNH^+$ | 832 | 825 | 817[d] | 824.8[e] |
| $CH_3CH_2OH$ | −220 | −238 | −234.8 ± 0.2 | −235.3 ± 0.5 |
| $CH_3CH_2OH_2+$ | 537 | 516 | 507[f] | 518.3[g] |
| $H_2O$ | −239 | −242 | −241.83 | −241.826 ± 0.040 |
| $C_2H_4$ | 59 | 50 | 52.2 ± 1 | 52.47 |

[a] Values are in kJ mol$^{-1}$. [b] Reference 30, 298 K values. [c] Reference 34, 298 K values. [d] Based on PA($CH_3CN$) = 787 kJ mol$^{-1}$. [e] Based on PA($CH_3CN$) = 779.2 kJ mol$^{-1}$. [f] Based on PA($CH_3CH_2OH$) = 788 kJ mol$^{-1}$. [g] Based on PA($CH_3CH_2OH$) = 776.4 kJ mol$^{-1}$.

(**VI**) and $[CH_3O(H)CH_3\cdots OH_2]^+$ (**VII**), which ultimately lead to the formation of the proton-bound dimer of dimethyl ether and water. [34−36]

An intermediate ion−dipole complex (**VIII**) similar to ion **VI** above for the methanol dimer has been located (Figure 4). This ion is calculated to lie 96 kJ mol$^{-1}$ above the proton-bound dimer at the G2(MP2,SVP) level of theory. So, an $S_N2$-type mechanism may be feasible for the isomerization of the proton-bound dimers of nitriles and alcohols. The dimer first rearranges to the complex **VIII**, which then undergoes the elongation of the C−$OH_2$ bond leading to isomers **IV** and **V**. This mechanism is also consistent with the isotopic labeling studies that show retention of the labels on the acetonitrile methyl group, the ethanol ethyl group and the bridging hydrogens.

**RRKM Calculations.** The G2(MP2,SVP) reaction surface was kinetically modeled with RRKM theory.[37] The microcanonical rate constant, $k(E)$, is a function of the density ($\rho$) and sum ($N^‡$) of states of the reacting ion and transition state, respectively. In its simplest form

$$k(E) = \frac{\sigma}{h}\frac{N^‡(E - E_0)}{\rho(E)}$$

where $E$ represents the internal energy of the reacting ion, $E_0$ is the 0 K activation energy, $\sigma$ is the symmetry number, and $h$ is Planck's constant. The sums and densities of states were calculated using the Beyer−Swinehart direct-count algorithm[37] employing scaled MP2/6-31+G(d) harmonic vibrational frequencies (Table 3). Rate constants were calculated employing the G2(MP2,SVP) 0 K activations energies. The resulting log $k(E)$ vs $E$ curves are presented in Figure 5.

There are six elementary reactions that need to be addressed: the reaction leading from **I** to $CH_3CNH^+ + CH_3CH_2OH$ ($k_1$), the reaction leading from **I** to $CH_3CH_2OH_2^+ + CH_3CN$ ($k_2$), the forward isomerization of **I** to **IV** ($k_3$), the dissociation of **IV** to **II** + $H_2O$ ($k_4$), the isomerization of **II** to **III** ($k_5$), and the dissociation of **III** to $CH_3CNH^+ + C_2H_4 + H_2O$ ($k_6$). The interconversion of **IV** and **V** is expected to be so fast that we have approximated the second potential well with ion **IV**. The

**TABLE 3: Vibrational Frequencies Used in the RRKM Analysis**

| species | harmonic vibrational frequencies ($cm^{-1}$)[a] |
|---|---|
| **I** | 6, 36, 51, 88, 125, 206, 266, 348, 349, 432, 543, 829, 837, 954, 1007,1028, 1074, 1075, 1130, 1227, 1296, 1344, 1452, 1457, 1480, 1503, 1504, 1533, 1543, 1561, 1764, 2273, 2289, 3113, 3120, 3170, 3201, 3222, 3222, 3222, 3257, 3663 |
| **II** | 19, 114, 156, 255, 295, 369, 480, 675, 820, 985, 1067, 1068, 1084, 1147, 1195, 1331, 1401, 1448, 1473, 1489, 1489, 1527, 1534, 1543, 2387, 3110, 3123, 3148, 3211, 3216, 3216, 3221, 3233 |
| **III** | 10, 70, 71, 132, 167, 183, 341, 348, 856, 878, 920, 969, 1027, 1052, 1076, 1076, 1084, 1269, 1403, 1448, 1485, 1485, 1515, 1682, 2218, 2946, 3111, 3199, 3210, 3216, 3216, 3291, 3313 |
| **IV** | 25, 58, 63, 118, 134, 167, 193, 268, 285, 304, 364, 375, 482, 683, 822, 987, 1064, 1075, 1097, 1151, 1197, 1333, 1403, 1438, 1470, 1491, 1503, 1530, 1535, 1549, 1716, 2398, 3114, 3124, 3148, 3210, 3216, 3221, 3228, 3237, 3719, 3843 |
| **TS(I → $CH_3CH_2OH_2^+$)** ($\Delta S^‡ = 14$ J $K^{-1}$ $mol^{-1}$) | (206),[b] 6, 18, 26, 44, 63, 266, 348, 349, 432, 543, 829, 837, 954, 1007, 1028, 1074, 1075, 1130, 1227, 1296, 1344, 1451, 1457, 1480, 1503, 1504, 1533, 1543, 1561, 1765, 2273, 2289, 3114, 3120, 3170, 3201, 3222, 3222, 3222, 3257, 3663 |
| **TS(I → $CH_3CNH^+$)** ($\Delta S^‡ = 14$ J $K^{-1}$ $mol^{-1}$) | (206),[b] 6, 18, 26, 44, 63, 266, 348, 349, 432, 543, 829, 837, 954, 1007, 1028, 1074, 1075, 1130, 1227, 1296, 1344, 1451, 1457, 1480, 1503, 1504, 1533, 1543, 1561, 1765, 2273, 2289, 3114, 3120, 3170, 3201, 3222, 3222, 3222, 3257, 3663 |
| **TS(I → IV)** ($\Delta S^‡ = -12$ J $K^{-1}$ $mol^{-1}$) | (1007),[b] 8, 55, 78, 134, 188, 206, 266, 348, 349, 432, 543, 829, 837, 954, 1028, 1074, 1075, 1130, 1227, 1296, 1344, 1451, 1457, 1480, 1503, 1504, 1533, 1543, 1561, 1765, 2273, 2288, 3114, 3120, 3170, 3201, 3222, 3222, 3222, 3257, 3663 |
| **TS(IV → II)** ($\Delta S^‡ = 14$ J $K^{-1}$ $mol^{-1}$) | (118),[b] 11, 27, 30, 56, 64, 193, 268, 285, 304, 364, 375, 482, 683, 822, 987, 1064, 1075, 1097, 1151, 1197, 1333, 1403, 1438, 1470, 1491, 1503, 1530, 1535, 1549, 1716, 2398, 3114, 3124, 3148, 3210, 3216, 3221, 3228, 3237, 3719, 3843 |
| **TS(III →** products) ($\Delta S^‡ = 14$ J $K^{-1}$ $mol^{-1}$) | (167),[b] 7, 38, 38, 68, 89, 341, 348, 856, 878, 920, 969, 1027, 1052, 1076, 1076, 1084, 1269, 1403, 1448, 1485, 1485, 1515, 1682, 2218, 2946, 3111, 3199, 3210, 3216, 3216, 3291, 3313 |
| **TS(II → III)** ($\Delta S^‡ = -70$ J $K^{-1}$ $mol^{-1}$) | 7, 61, 61, 162, 217, 265, 349, 361, 762, 871, 939, 1077, 1077, 1206, 1248, 1279, 1322, 1386, 1459, 1508, 1508, 1519, 1610, 2231, 2637, 3120, 3203, 3220, 3221, 3238, 3307, 3358 |

[a] MP2/6-31+G(d) frequencies scaled by 0.9434 as recommended by Scott and Radom.[7] [b] Corresponds to the vibrational mode that most closely matches the dissociation reaction.

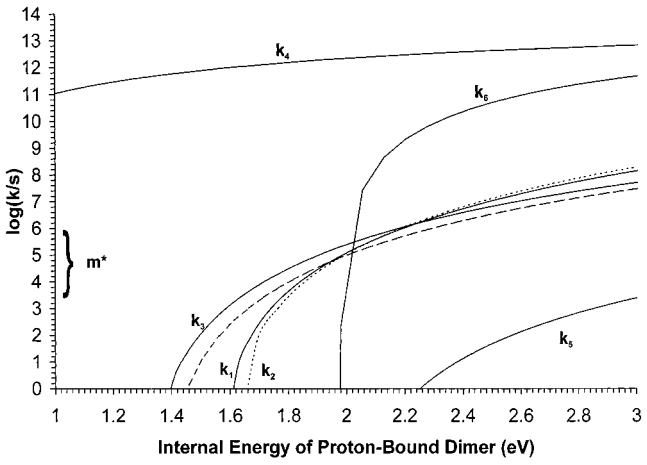


**Figure 5.** Plot of log $k(E)$ vs ion internal energy curves for the six elementary reactions of $(CH_3CN)(CH_3CH_2OH)H^+$ (all energies are referred to the ground state of the proton-bound dimer): $k_1$: the reaction leading from **I** to $CH_3CNH^+ + CH_3CH_2OH$; $k_2$: the reaction leading from **I** to $CH_3CH_2OH_2^+ + CH_3CN$; $k_3$: the forward isomerization of **I** to **IV** empolying an $E_0$ of 130 kJ $mol^{-1}$; $k_4$: the dissociation of **IV** to **II** + $H_2O$; $k_5$: the isomerization of **II** to **III**; $k_6$: and the dissociation of **III** to $CH_3CNH^+ + C_2H_4 + H_2O$. A dashed line represents $k_3$ using an $E_0$ of 135 kJ $mol^{-1}$. The region m* denotes the range of rate constants responsible for observations in the 2FFR of the instrument.

reverse isomerization of **IV** to **I** was not considered because the dissociation of **IV** to **II** + $H_2O$ will be the dominant process for ion **IV** (Figure 5). This is consistent with the observation from the isotopic labeling studies that no mixing of the acetonitrile-methyl hydrogens occurs in the labeled clusters. The conversion of **II** to **III** ($k_5$) was modeled with the ab initio transition structure **TS(II → III)**. The $\Delta S^‡$(600 K) for this process is $-70$ J $K^{-1}$ $mol^{-1}$, and thus the log $k(E)$ vs $E$ curve rises only gradually with increasing internal energy (Figure 5). For the dissociation reaction channels leading from the proton-bound dimer to products, the vibrational frequencies for the transition states were modeled using those of ion **I**, less one mode that most closely matched the dissociation reaction (206 $cm^{-1}$). In addition, the very small vibrational frequency in ion **I** due to hindered internal rotation about the hydrogen bond (6 $cm^{-1}$) was not included in the $\rho(E)$ and $N^‡(E - E_0)$ calculations as a distinct vibration; rather it was treated as a hindered internal rotor with a rotational constant of 19.7 GHz. To achieve a suitably loose transition state, the lowest five TS frequencies were scaled to obtain an entropy of activation, $\Delta S^‡$(600 K), of 14 J $K^{-1}mol^{-1}$. This value is typical for simple bond cleavage reactions. It was noted earlier that the two dissociation reactions from ion **I** leading to $CH_3CNH^+$ and $CH_3CH_2OH_2^+$ may be characterized by different $\Delta S^‡$ values. Increasing the $\Delta S^‡$(600 K) from +14 to +20 J $K^{-1}$ $mol^{-1}$ for the protonated ethanol channel leads to log $k(E)$ vs $E$ curves that cross in the metastable internal energy window (Figure 5). This modest difference in $\Delta S^‡$ may explain the similarity of the two signals in the MI mass spectrum and the inversion in intensity in the CID mass spectrum.

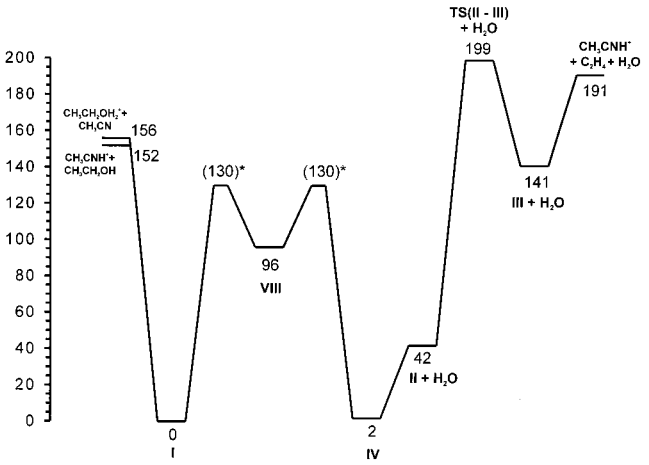


**Figure 6.** Theoretical reaction profile for $(CH_3CN)(CH_3CH_2OH)H^+$. Relative energies calculated at G2(MP2,SVP) except for the barrier to isomerization from **I** → **IV**, which was obtained from the kinetic modeling of the forward isomerization reaction (see text). All values are in kJ mol$^{-1}$.

The isomerization of **I** to **IV** was modeled in a fashion similar to that discussed above. Without an ab initio transition structure, the entire $S_N2$-type reaction was modeled with a single set of frequencies. The transition state, **TS(I → IV)**, frequencies chosen were those for **I**, less one mode at 1007 cm$^{-1}$, to represent the motion over the col on the reaction surface. In this case, the low vibrational frequency in **I** of 6 cm$^{-1}$ was included in the $\rho(E)$ of **I** and a scaled value included for the $N^{\ddagger}$ of the transition state. The lowest five frequencies were then scaled to achieve a $\Delta S^{\ddagger}$(600 K) value of $-12$ J K$^{-1}$ mol$^{-1}$. The unknown quantity in this process is the activation energy. However, since the isomerization competes with the dissociation to $CH_3CH_2OH_2^+ + CH_3CN$ and $CH_3CNH^+ + CH_3CH_2OH$ on the microsecond time scale, (the MI spectrum), the $E_0$ for the isomerization can be adjusted to produce the desired overlapping log $k(E)$ vs $E$ curves (Figure 5). The estimate that this provides for the activation energy for this reaction is 130 kJ mol$^{-1}$. It is important to keep in mind the qualitative nature if this modeling. The segment of the internal energy distribution of the dimer ion responsible for observations in the second-field free region of the mass spectrometer is governed by the time scale of the instrument.[38] However, the estimated frequencies used in the RRKM calculation, and the modeling of the isomerization of **I** to **IV** with a single transition state, all lead to uncertainties in this value of the isomerization activation energy. It is still valuable, though, to be able to place an approximate value on this process.

*Reaction Mechanism* The reaction surface that the experimental and theoretical evidence suggests is shown in Figure 6. This surface is qualitatively similar to that presented in Figure 1 for the methanol-acetonitrile system. One key difference is in the height of the isomerization barrier for the initially generated proton-bound dimer. In the present system, this barrier lies approximately 22 kJ mol$^{-1}$ below the lowest dissociation threshold ($CH_3CNH^+ + CH_3CH_2OH$), while in the previous case it was only 6 kJ mol$^{-1}$ lower. So, isomerization is more facile in the $(CH_3CN)(CH_3CH_2OH)H^+$ ion. This is at least consistent with an $S_N2$ nature of the isomerization process. The larger alkyl group may mean a weaker C−O bond in the intermediate ion **VIII**. The larger alkyl group present in the current system also results in greater charge stabilization and thus lower energy intermediates. The greater charge stabilization can also lower the energy of transition structures. We are currently exploring the dimers involving propanols and butanols to determine the extent to which this hypothesis may be extended to larger systems.

## 5. Conclusion

In this study, the unimolecular chemistry of low internal energy $(CH_3CN)(CH_3CH_2OH)H^+$ ions has been investigated by tandem mass spectrometry and ab initio theory. The ions undergo competing dissociation and isomerization reactions on the microsecond time scale. Two simple bond-cleavage reactions to produce $CH_3CNH^+ + CH_3CH_2OH$ and $CH_3CH_2OH_2^+ + CH_3CN$ compete with an isomerization to $(CH_3CNCH_2CH_3^+)(H_2O)$. This isomeric form of the proton-bound dimer is responsible for the loss of water to form $CH_3CNCH_2CH_3^+$. The barrier for the isomerization was estimated from RRKM calculations to lie 22 kJ mol$^{-1}$ below the lowest energy dissociation products $CH_3CNH^+ + CH_3CH_2OH$. This is significantly lower than that found in an earlier examination of the acetonitrile−methanol proton-bound dimer in which the isomerization barrier leading to water loss was found to lie only 6 kJ mol$^{-1}$ lower than the simple dissociation products. A possible explanation is that the isomerization occurs via an $S_N2$ type mechanism involving intermediate ion−dipole complexes, at least one of which was found in the present study and found to lie 96 kJ mol$^{-1}$ above the proton-bound dimer. The polarizability of the alkyl group is an important factor in determining the energy requirement for the isomerization.

**Acknowledgment.** P.M.M. thanks the Natural Sciences and Engineering Research Council of Canada for financial support, and the University of Ottawa for a grant toward the purchase of a computer workstation. The authors also thank the High Performance Computing Centres at the University of Montreal and Queen's University for generous donations of computing time.

## References and Notes

(1) Yates, B. F.; Bouma, W. J.; Radom, L. *Tetrahedron* **1986**, *22*, 6225.
(2) Harnish, D.; Holmes, J. L. *J. Am. Chem. Soc.* **1991**, *113*, 9729.
(3) Morton, T. H. *Org. Mass Spectrom.* **1991**, *26*, 18.
(4) Heinrich, N.; Schwarz, H. In *Ion and Cluster Ion Spectroscopy*; Elsevier: Amsterdam, 1989.
(5) Schaftenaar, G.; Postma, R.; Ruttink, P. J. A.; Burgers, P. C.; McGibbon, G. A.; Terlouw, J. K. *Int. J. Mass Spectrom. Ion Processes* **1990**, *100*, 521.
(6) Holmes, J. L.; Hop, C. E. C. A.; Terlouw, J. K. *Org. Mass Spectrom.* **1986**, *21*, 776.
(7) Booze, J. A.; Baer, T. *J. Phys. Chem.* **1992**, *96*, 5715.
(8) Mayer, P. M.; Baer, T. *J. Phys. Chem.* **1996**, *100*, 14949.
(9) Mazyar, O. A.; Mayer, P. M.; Baer, T. *Int. J. Mass Spectrom. Ion Processes* **1997**, *167/168*, 389.
(10) Szulejko, J. E.; McMahon, T. B. *Org. Mass Spectrom.* **1993**, *28*, 1009.
(11) Aviyente, V.; Iraqi, M.; Peres, T.; Lifshitz, C. *J. Am. Soc. Mass Spectrom.* **1991**, *2*, 113.
(12) Audier, H. E.; Monteiro, C.; Mourgues, P.; Robin, D. *Rapid Commun. Mass Spectrom.* **1989**, *3*, 84.
(13) Beauchamp, J. L.; Caserio, M. C. *J. Am. Chem. Chem.* **1972**, *94*, 2638.
(14) Beauchamp, J. L.; Caserio, M. C.; McMahon, T. B. *J. Am. Chem. Soc.* **1974**, *96*, 6243.
(15) Mafune, F.; Kohno, J.; Kondow, T. *J. Phys. Chem.* **1996**, *100*, 10041.
(16) Zhang, X.; Yang, X.; Castleman, A. W. *Chem. Phys. Lett.* **1991**, *185*, 298.
(17) Feng, W. Y.; Iraqi, M.; Lifshitz, C. *J. Phys. Chem.* **1993**, *97*, 3510.
(18) Feng, W. Y.; Lifshitz, C. *Int. J. Mass Spectrom. Ion Processes* **1995**, *149/150*, 13.
(19) Mayer, P. M. *J. Phys. Chem. A* **1999**, *103*, 3687.
(20) Holmes, J. L.; Mayer, P. M. *J. Phys. Chem.* **1995**, *99*, 1366.
(21) Busch, K. L.; Glish, G. L.; McLuckey, S. A. *Mass Spectrometry/Mass Spectrometry*; VCH Publishers: New York, 1988.

(22) Hehre, W. J.; Radom, L.; Schleyer, P. v. R.; Pople, J. A. *Ab Initio Molecular Orbital Theory*; Wiley: New York, 1986.

(23) Frisch, M. J.; Trucks, G. W.; Schlegel, H. B.; Gill, P. M. W.; Johnson, B. G.; Robb, M. A.; Cheesman, J. R.; Keith, T.; Petersson, A.; Montgomery, A.; Raghavachari, K.; Al-Laham, M. A.; Zakrzewski, V. G.; Ortiz, J. V.; Foresman, J. B.; Cioslowski, J.; Stefanov, B. B.; Nanayakkara, A.; Challacombe, M.; Peng, C. Y.; Ayala, P. Y.; Chen, W.; Wong, M. W.; Andres, A. L.; Replogle, E. S.; Gomperts, R.; Martin, R. L.; Fox, D. J.; Binkley, J. S.; Defrees, D. J.; Baker, J.; Stewart, J. P.; Head-Gordon, M.; Gonzalez, C.; Pople, J. A. *GAUSSIAN 94* (Rev. E.1); Gaussian, Inc.: Pittsburgh, 1995.

(24) Frisch, M. J.; Trucks, G. W.; Schlegel, H. B.; Scuseria, G. E.; Robb, M. A.; Cheeseman, J. R.; Zakrzewski, V. G.; Montgomery, J. A.; Stratmann, R. E.; Burant, J. C.; Dapprich, S.; Millam, J. M.; Daniels, A. D.; Kudin, K. N.; Strain, M. C.; Farkas, O.; J. Tomasi; Barone, V.; Cossi, M.; Cammi, R.; Mennucci, B.; Pomelli, C.; Adamo, C.; Clifford, S.; Ochterski, J.; Petersson, G. A.; Ayala, P. Y.; Cui, Q.; Morokuma, K.; Malick, D. K.; Rabuck, A. D.; Raghavachari, K.; Foresman, J. B.; Cioslowski, J.; Ortiz, J. V.; Stefanov, B. B.; Liu, G.; Liashenko, A.; Piskorz, P.; Komaromi, I.; Gomperts, R.; Martin, R. L.; Fox, D. J.; Keith, T.; Al-Laham, M. A.; Peng, C. Y.; Nanayakkara, A.; Gonzalez, C.; Challacombe, M.; Gill, P. M. W.; Johnson, B.; Chen, W.; Wong, M. W.; Andres, J. L.; Gonzalez, C.; Head-Gordon, M.; Replogle, E. S.; Pople, J. A. *GAUSSIAN 98* (Rev. A.7).; Gaussian Inc.: Pittsburgh, PA, 1998.

(25) Mayer, P. M. *J. Chem. Phys.* **1999**, *110*, 7779.

(26) Mayer, P. M. *J. Phys. Chem. A* **1999**, *103*, 5905.

(27) Mayer, P. M. *Chem. Phys. Lett.* **1999**, *314*, 311.

(28) Curtiss, L. A.; Redfern, P. C.; Smith, B. J.; Radom, L. *J. Chem. Phys.* **1996**, *104*, 5148.

(29) Scott, A. P.; Radom, L. *J. Phys. Chem.* **1996**, *100*, 16502.

(30) Lias, S. G.; Bartmess, J. E.; Liebman, J. F.; Holmes, J. L.; Levin, R. D.; Mallard, W. G. *J. Phys. Chem. Ref. Data* **1988**, *17* (Suppl.1).

(31) Hunter, E. P.; Lias, S. G. *J. Phys. Chem. Ref. Data* **1998**, *27*.

(32) Holmes, J. L.; Aubry, C.; Mayer, P. M. *J. Phys. Chem. A* **1999**, *103*, 705.

(33) Burgers, P. C.; Holmes, J. L. *Int. J. Mass Spectrom. Ion Processes* **1984**, *58*, 15.

(34) Raghavachari, K.; Chandrasekhar, J.; Burnier, R. C. *J. Am. Chem. Soc.* **1984**, *106*, 3124.

(35) Sheldon, J. C.; Currie, G. J.; Bowie, J. H. *J. Chem. Soc., Perkin Trans. 2* **1986**, 941.

(36) Bouchoux, G.; Choret, N. *Rapid. Commun. Mass Spectrom* **1997**, *11*, 1799.

(37) Baer, T.; Hase, W. L. *Unimolecular Reaction Dynamics, Theory and Experiments*; Oxford University Press: New York, 1996.

(38) Holmes, J. L.; Aubry, C. A.; Mayer, P. M. *J. Phys. Chem.* **1999**, *103*, 705.